Iranian Journal of Basic Medical Sciences

ijbms.mums.ac.ir

IJBMS

Development of specific nanobodies (VHH) for CD19 immuno-targeting of human B-lymphocytes

Seyed Reza Banihashemi [1], Ahmad Zavaran Hosseini [1]*, Fatemeh Rahbarizadeh [2], Davoud Ahmadvand [3]

[1] Department of Medical Immunology, Faculty of Medical Sciences, Tarbiat Modares University, Tehran, Iran
[2] Department of Medical Biotechnology, Faculty of Medical Sciences, Tarbiat Modares University, Tehran, Iran
[3] Department of Medical Biochemistry, Faculty of Applied Medical Sciences, Iran University of Medical Sciences,Tehran, Iran

ARTICLE INFO

Article type:
Original article

Article history:
Received: Oct 9, 2017
Accepted: Sep 28, 2017

Keywords:
CD19
Drug delivery system
Lymphoma
Nanobody
Phage display

ABSTRACT

Objective(s): CD19 is a transmembrane glycoprotein of immunoglobulin superfamily. In order to treat lymphoma, monoclonal antibodies (mAb) can target different antigens, including CD19, CD20 and CD22 on the surface of B-cells. Along with biotechnology progress, a new generation of antibodies is introduced, with the purpose of eliminating the defects of the previous generation. Among the most developed one are nanobodies (Nb). Nbs are a unique kind of camelid single domain antibody fragments with a broad range of medical applications. Unique physicochemical properties of Nbs have made them ideal candidates for therapeutic and diagnostic applications.

Materials and Methods: An immune gene library was created, and several CD19 specific Nbs were selected through antigen panning process, and their molecular properties as well as specificity, sensitivity, affinity and immunoreactivity against CD19 positive and negative cells were evaluated.

Results: The Nb library was prepared with 7.2 x107 members. We managed to isolate a panel of CD19-specific Nbs after the last round of selection with the affinity of isolated Nbs being estimated at the standard range of 15-35 nM. Sequence analysis of positive clones was indicative of the fact that 12 variable sequences were confirmed. Of all these 12 clones, 2 clones with the greatest level signal in ELISA underwent subsequent analysis. Our sequencing results indicated high sequence homology (approximately 90%) between the Nb and Homa variable immunoglobulin domains.

Conclusion: Specific Nbs possess the potential to be used as novel therapeutic approaches in order to treat autoimmune diseases and B-cell lymphoma.

► *Please cite this article as:*
Banihashemi SR, Zavaran Hosseini A, Rahbarizadeh F, Ahmadvand D. Development of specific nanobodies (VHH) for CD19 immuno-targeting of human B-lymphocytes. Iran J Basic Med Sci 2018; 21:455-464. doi: 10.22038/IJBMS.2018.26778.6557

Introduction

CD19 is a transmembrane glycoprotein of the immunoglobulin superfamily (IgSF) (1). CD19 is expressed by both normal and malignant B-cells as well as dendritic cells, and it is an important and effective biomarker (2). The study of knockout and transgenic mouse models of CD19 shows that CD19 plays a critical role in maintaining the balance between antigen-induced and humoral responses, and reveals induced tolerance (3). For the treatment of lymphoma, different monoclonal antibodies (mAb) have been utilized that are selective for various antigen on the outer surface of B cells (4). Among those, Rituximab can target the CD20 on the outer layer of B-cells and it is one of mAbs that has revolutionized the treatment of lymphoma (5). However, due to the lack of expression of CD20 on the surface of B-cell lineage including plasma cells, there is an urgent need for an alternative antigen target (6). CD19 is one of the proposed alternatives for CD20 (7). Due to the expression of CD19 on B-cells lineages, many studies have recently focused on this antigen as a cancer-specific biomarker (8). Hence, several research centers have put significant effort and investment on designing and producing a novel mAb, which can be used against CD19 antigen (9). These efforts are focused on developing therapeutic targets against B-cell malignancies. Malignancies that are caused by lack of B-cell efficiency are very wide ranging and dangerous(10).

Successful preclinical research has paved the way for the clinical trials, mainly based on the first generation of immunoconjugated mouse anti-CD19 toxin, but due to poor biochemical reactants and human anti-murine antibody (HAMA) generation most of these trials ended up in failure (11). These problems have had a considerable limiting influence on the clinical practice, culminating in the emergence and production of a new generation of antibodies. Based on the novel structure and functional properties of naturally–occurring heavy chain-only antibodies (12), derived nanobodies (Nbs) are a unique kind of camelid single domain antibody fragments with a broad range of medical applications (13). The heavy chain antibodies of camel were first discussed by Ungar-Waroni *et al.* who demonstrated many Ig-Like proteins in dromedary serum and proved their significance in the process of passive immunity transmission from dam to calf through colostrum (14). Heavy chain antibodies include an antigen-binding region, VHH and two constant domains. Sufficient data is available on genetic elements of Nbs, yet *in vivo* production process of these molecules is still ambiguous.

**Corresponding author:* Ahmad Zavaran Hosseini. Department of Medical Immunology, Faculty of Medical Sciences, Tarbiat Modares University, Tehran, Iran. Tel: +98-82883601; Email: zavarana@modares.ac.ir

Until this moment, only three secondary functional IgGm serum of Camelidae have been identified: IgG_1 can be defined as a heterodimer, which consists of homodimers with heavy and light chains. On the other hand, IgG_2 and IgG_3 consist of merely heavy chains. As a result, they may be considered as famous heavy chain antibodies (hcAbs) (14,15). The Nbs resistance to severe conditions makes them suitable entities for administration via different routes (topical, oral or respiratory)(16).

Besides genetic map of the single variable domain VHH that binds to antigen, in order to produce Nbs with high affinity, among isolated B-cells, activated clones against the target antigen (CD19) must be identified following immunization of a camel (17). A common method to achieve this goal is via phage display through which the antigen is expressed on the phage surface *in vitro* and then the favorable clone is isolated by consecutive panning (18).

The present research has sought to create an immune gene library from camel and to select and validate the specific Nbs against CD19 on human B-cells with the aid of phage display technology.

Materials and Methods

Antigens and antibodies

Recombinant human CD19 protein was purchased from Abcam (Cambridge, UK). The anti-M13 horseradish peroxidase (HRP) conjugated antibody and HRP-linked anti-mouse IgG produced in goat were provided from Sigma-Aldrich (St Louis, MO, USA). The mouse HRP and fluorescein isothiocyanate (FITC)-linked monoclonal anti-His tag antibodies were obtained from Abcam (Cambridge, MA). The Human CD19 mAb conjugated to PE was purchased from Abcam (Cambridge, MA). Finally, the pCom3XSS vector was purchased from Addgene (Cambridge, MA).

Bacterial strains and culture media

Escherichia coli (*E. coli*) XL1-Blue (Merck, Germany) was considered appropriate for the purpose of phage display design and it was cultivated in Luria– Bertani (LB) and 2XYT growth mediums, supplemented with 100 µg/ml ampicillin. *E. coli* TAP10F (Thermo Fisher,USA) was utilized for Nb expression. TAP10F was grown in SB medium, supplemented with 100 µg/ml ampicillin and 50 mM MgCl2 (19).

Cell lines and conditions of cultivation

B cell lines Raji, Ramos, Namalwa and Daudi (CD19 Positive) and K506 (CD19 Negative) were purchased from the national cell bank of Iran (Pasture Institute of Iran, Tehran, Iran) and cultured in RPMI 1640 (Gibco, USA), supplemented with 10 % (v/v) heat-inactivated fetal bovine serum, 2 mM L-glutamine, 0.4 mM sodium pyruvate, 100 U/ml penicillin, and 100 µg/ml streptomycin (Gibco, Scotland, UK). Respective cell lines were cultured in similar conditions (80% humidity, 5% CO2 at 37 ˚C)(19).

VHH amplification and library construction

Two relatively young female camels were given six intramuscular and intradermal Namalwa injections every three weeks. About 10^6 cells/ml supplemented with 2 ml Freunds complete adjuvant were utilized for the first injection. Booster immunization was performed using 10^6 Namalwa cells/ml along with Freund incomplete adjuvant. The last injection was performed with 10^6 Namalwa cells/ml and no adjuvant. Eight days following the sixth injection, a blood sample (about 250 ml) of the subjects was obtained from the immunized camels and the peripheral blood lymphocytes were isolated by centrifugation on a Ficoll (Sigma-Aldrich) discontinuous gradient. Total RNA was extracted from the peripheral blood lymphocytes (Nucleo Spin RNA II, Qiagen, USA) and first strand cDNA was synthesized from total or polyA+RNA, using Prime Script RTase, a M-MLV (Moloney Murine Leukemia Virus)-derived reverse transcriptase (TAKARA, Japan). Then, the gene fragments encoding Nbs were amplified by nested PCR. In order to amplify VHH, a nested PCR was designed. The first PCR sought to amplify the fragments between framework 1 and regions correlating to CH2, using five sets of specific primers including CALL001: 5'-GTC CTG GCT CTC TTC TAC AAG G-3'; CALL002: 5'-GGT ACG TGC TGT TGA ACT GTT CC-3'; VHBACKA6: 5'- GAT GTG CAG CTG CAG GCG TCT GG(A/G) GGA GG-3'; and CH2FORTA4: 5'-CGC CAT CAA GGT ACC AGT TGA-3'. Fragments (600 and 700 bp) driven from heavy chain antibodies were extracted from agarose gel using a kit designed for gel purification (Invitrogen, USA). They were subsequently utilized as templates for the second round of PCR. VHH was amplified using four specific degenerated VHH primers including VHH-F: 5'- CTGGCCCAGGCGGCCGAGGTGCAGCTG(C/G) (A/T) G(C/G) A (G/T) TC (G/T) G-3'; and VHH-R primer: 5'-ACTGGCCGGCCTGGCCTGAGGAGACGGTGATGACC (A/T) GGGTC-3'. These primers were bound to regions corresponding to framework 1 and framework 4. VHH fragments were purified from agarose gel and cloned into a *sfi*I digested pComb3xSS phagemid vector. Amplified Nb products were digested with *sfi*I (Thermo Scientific, USA) and the resulting fragments were ligated into phagemid vector pComb3x SS. The ligation compound was transformed into *E. coli* XL1-Blue via electroporation (2500 v, 5 msec in a 0.2 mm covet) and put on LB plates, which contained ampicillin. This library (Nb repertoire) was expressed on phages after infection with 10^{12} to 10^{13} plaque/ml M13KO7 helper phage (Thermo Scientific-USA) and the phages were isolated through precipitation using PEG 8000 to 4% w/v and 6 g of sodium chloride to 3% w/v (19-21).

Selection of the CD19 binding nanobodies via antigen panning

Biopanning was used to isolate favorable clones in the library. In this regard, a 6-wells plate was coated with the CD19 antigen (25 ng/well) or bovine serum albumin (BSA; 500 ng/ml, for subtractive panning) in a temperature of 4 ˚C overnight. Binding of respective Nb-carrying phages to the coated wells was accomplished through five rounds of panning. The wells were rinsed twice using phosphate buffered saline (PBS) and then blocked by PBS containing 2 % (w/v) ELISA-grade BSA and 1 % (w/v) skimmed milk at 37 ˚C for 2 hr. The phage particles (about 3 $\times 10^{12}$ transducing units) aspirated with the blocking solution in a total volume of 2 ml of PBS with 4 % BSA and pre-incubated on the BSA-coated wells at 37°C for 2 hr (to aspirate non-specific

binders) and then transferred to the CD19-coated wells. After incubation at 37°C for 3 hr, the supernatants were aspirated and the wells were washed four times with 0.5 % Tween 20 in PBS (PBST) and twice with PBS alone. After shaking out of the final washing solution, 500 µl of freshly prepared 1 mg/ml trypsin in TBS was added to every single well. For the next rounds of panning, the eluted phages were amplified by infecting log-phase *E. coli* XL1-Blue cells followed by their super-infection with the helper phage, as detailed above. In addition, input and output phages were titrated by infecting the log-phase XL1-Blue competent cells using an aliquot of phage particles and then the samples were plated out on LB-ampicillin plate. Five consequent rounds of panning were carried out and the intensity of selection was increased with each phase using increasing Tween concentrations (0.5–10%) in the washing step (19, 20, 22, 23).

Polyclonal phage ELISA

The improvement of the selection process can be accomplished through different methods such as polyclonal phage ELISA. Polyclonal phage ELISA and polyclonal phage cell ELISA wherein the phage pools are produced at the end of each stage of panning were examined with phages from the unplanned library. In polyclonal phage ELISA, CD19 antigen (20 ng/well) and BSA (500 ng/ml), as negative control in PBS (pH 7.2), were used to coat the wells of microtiter plate and incubated overnight at 4 ˚C. After rinsing with PBS twice, the wells were blocked with 1% skimmed milk and 2% BSA/PBS for 2 hr at 37 ˚C. Then, the blocking buffer was aspirated and 10^{12} transducing units of antigen panning output phages were added and incubated for 4 hr at 37 ˚C. After five rounds of washing steps using PBST, 100 µl of the anti-M13 antibody conjugated to HRP (1/1000) were supplemented and incubated for 4 hr at 37 ˚C. Subsequently, the plate was rinsed five times using PBST and PBS and the peroxidase enzyme activity was detected by adding 70 µl of 3, 3′, 5, 5′-tetramethylbenzidine (TMB) as substrate. The reaction was blocked by the addition of 50 µl of 1 M H_2SO_4 to the confluent cells in 96-well cell culture plates. In an attempt to preserve the original structure of the CD19 antigen on the Namalwa cells and to prevent the cell lysis, all the procedures were conducted at 4 ˚C. Subsequently, the wells were depleted and pre-incubated with 3% BSA/PBS on ice for 30 min, in order to eliminate non-specific binding, followed by 1 hr incubation with 10^{12} transducing units of cell-panning output phages on ice. After the incubation time, the wells were washed with 1% BSA/PBS and the assay was operated as explained previously (20, 21).

Selection of CD19-specific phage nanobodies and DNA sequencing

The antigen-specific phage clones were recognized by monoclonal phage ELISA using the anti-M13 mAb. As many as 800 randomly nominated single clones were selected from output phages and the antigen was analyzed using ELISA and PCR, for their binding capacity to the CD19, in order to detect the VHH sequence as discussed previously. The clones were dimmed positive when the optical density (OD) of 450 nm, measured for CD19-coated wells was around three times of baseline of BSA-coated wells. The clones with positive phage were isolated, characterized and sequenced to identify the novel Nb. An algorithm was utilized to produce a tree from given distances (or dissimilarities) between sequences (Neighbour-joining phylogenetic options and distance Gishin model)(24-26).

Production of soluble nanobodies

In order to produce soluble Nbs, phages picked in monoclonal phage ELISA were utilized for infection of non-suppressive strain TAP10F. Transformants were developed in 1 L SB containing 100 µg/ml ampicillin, while they were shaken at 250 rpm at 37 ˚C.The process of protein expression was induced at OD 0.8 using 0.5 mM isopropyl-b-D-thiogalactopyranoside (IPTG) and the culture was incubated for 24 hr in a temperature of 24 to 27 ˚C. After incubation, the bacterial pellet was resuspended in PBS, containing 1 mM of the protease inhibitor phenylmethylsulfonyl fluoride (PMSF) and sonicated. The cell debris was centrifuged at 14,000 rpm at 4 ˚C for 45 min in order to isolate the transparent and clear supernatant, which contains soluble Nbs that are expressed. The 6× His-tagged Nbs were purified by chromatography, utilizing Ni-NTA resin (Qiagen, USA). The elution was then rinsed using four sample volumes of PBS, containing protease inhibitor using a centriprep 5 filtration system, which has an MW cut-off of 5 kDa. Protein concentration was measured using Bradford assay. Purified Nbs were used for further specification or stored in at -20 ˚C (19, 27, 28).

SDS-PAGE and Western blot analysis

In order to confirm the molecular weight of the soluble Nbs, expressed by the specific positive clones, protein samples were electrophoresed using a reducing sodium dodecyl sulfate polyacrylamide gel (SDS-PAGE) and transferred onto a nitrocellulose membrane by electroblotting. After the membrane was blocked with 2% BSA in TBS for 2 hr at 37 ˚C, it was probed using HRP-conjugated anti-HA antibody, diluted in TBS containing 0.1% BSA. The membranes were washed three times with TBS-T and twice with TBS and then visualized using 4-chloro-1-naftol substrate (29) .

Analysis of the soluble nanobody reactivity towards the purified CD19

Each selected Nb (2 µg/ml) was incubated in triplicate at 37 ˚C for 1 hr in a microtiter plate coated with the CD19 antigen and BSA (as negative control) and blocked with 1% BSA and 3% skimmed milk. Having rinsed it three times using TBS-T, 100 µl anti-HA antibody conjugated to HRP (diluted 1/10000 in TBS containing 0.1% BSA) was supplemented and the resulting mixture was incubated at 37 ˚C for 2 hr. After washing with TBS-T and TBS, TMB substrate was added, the color of the reaction was detected and the absorbance intensity was measured at 450 nm (30).

Analysis of binding specificity

The individual Nbs were tested to measure their specificity and possible cross-reactivity with structurally relative compounds such as casein, porcine submaxillary mucin (PSM), skimmed milk, BSA, HER2, VHH and Endoline. Several types of antigens were

coated in microtiter plates (1 µg/ml) and tested with different concentrations of anti-CD19 Nb (31).

Analysis of binding sensitivity

In an attempt to come up with more detailed characterization of the selected Nb fragments, ELISA was conducted by reducing the amount of the coated CD19 antigen. A range of antigen concentrations (0, 6.25, 12.5, 25 and 50 ng/ml) was prepared in PBS buffer and coated in microtiter plates at 4 ˚C overnight. Subsequently, different soluble Nbs (2 µg/ml) were added and the bound antibodies were determined using HRP-labeled anti-HA antibody(19, 32) .

Analysis of competitive binding

A competitive binding assay was carried out to assess binding of the nominated Nbs to the soluble antigen. All rounds of this test were carried out similar to the analysis of the soluble Nb reactivity, with the exception that the Nb solutions were pre-incubated with serial dilutions of soluble CD19 antigen (up to 20 ng/ml) for 2 hr before they were added to the wells. Bound antibodies were monitored by HRP-labeled anti-HA antibody (20).

Affinity determination

The affinity constant determination of the nominated Nbs was performed using the non-competitive enzyme immunoassay described by Beatty *et al*. The microtiter plates were coated using 100 µl of two different concentrations (10 and 100 ng/ml) of the CD19 antigen in BSA, and incubated at 4 ˚C for one night. The wells were blocked with 1% BSA in 250 µl TBS and then incubated with different concentrations of soluble Nbs (10–40 nM) for 2 hr at 37°C. The bound Nbs were detected using HRP-conjugated anti-HA antibody and the signal intensities were measured at 450 nm. The affinity of the Nb was estimated at the concentration yielding half-maximum binding to CD19 antigen(19, 33).

Analysis of nanobody reactivity by cell ELISA

Cell ELISA was designed to study the reactivity of single soluble Nbs as well as the Nb mixture with Namalwa and K506 cell lines. In this setting, the 3% BSA/PBS solution acted as a negative control. Both cell lines were developed up to level of confluency on 96-well cell culture plates. Soluble Nbs were then added to each well and processed as discussed above in polyclonal phage cell ELISA, with the exception of using anti-HA mAb instead of HRP linked to anti-M13 antibody (19, 20).

Flow cytometry studies

Fluorescence-activated cell sorting (FACS) experiments were conducted to determine the binding of SRB-37 and SRB-38 to K562, Raji, Ramos, Daudi and Namalwa cells. For this purpose, 1×10^6 cells in the exponential growth phase were seeded in sterile tubes. Cells were incubated with Nbs for 2 hr at 4 ˚C, and then they were rinsed using cold PBS. Binding of Nbs was analyzed in a Becton Dickinson FACScan (BD Biosciences, USA), after labeling with mouse anti-His mAb. The binding of Nbs to Raji, Ramos, Daudi, Namalwa and K562 cells was characterized by rightward shifts in the fluorescence peak. Commercial anti-CD19-PE (BD Biosciences, USA) were used to demonstrate the expression of CD19 on the cell lines (34).

Statistical analysis

Various experimental groups were compared against others using the Kruskal–Wallis test. The Mann–Whitney test was conducted to define the statistical significance of the differences between two various statuses. The software used for the statistical analysis was Stata 3 for windows. A *P-value* of less than <0.05 was considered to be statistically significant. The phylogenetic tree was produced using BLAST pairwise alignments, and Max sequence difference >0.5 for sequence grouping was considered accurate.

Results

Constriction and enrichment of the phage-displayed CD19 binding nanobodies

Mononuclear cells were separated from heparinized blood of an immunized camel. Total RNA was extracted from 10^6 cells and reverse transcribed to cDNA, and subsequently used as the PCR template. The amplified fragments were extracted from classical antibody (900 bp) and the CH2-located regions and framework 1 were amplified (heavy chain antibody) (600-700 bp) (Figure 1a). In the second round of PCR, the VHH fragments (400 bp) were amplified with specific primers that bind to framework 1 and framework 4 and the variable region (Figure 1b). *Sfi*1-digested vector and VHH were ligated to form the final fragment (Figure 1c). Finally, the Nb library was prepared with as many as 7.2 $x10^7$ members.

Nb-expressing phages were obtained from the immune library following superinfection with M13KO7. In order to enrich specific Nbs against CD19, five rounds of biopanning were conducted on purified CD19 antigen. Since enforcing more rounds of selection in panning leads to a remarkable decrease in specificity of the phages, panning was accomplished in five cycles. Titration of each stage showed a measured increase in the output/input ratio of phage particles following each round of panning, demonstrating the developing enrichment of the CD19-specific clones during the primary rounds of panning (Table 1). This ratio increased by 20 fold following the fifth biopanning round. Analysis

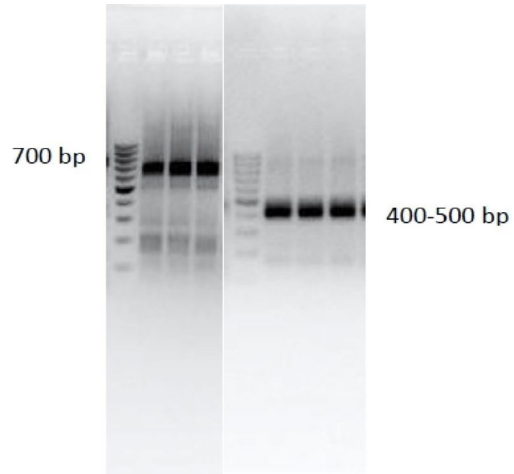

Figure 1. library construction. (a) First PCR product analysis by agarose gel electrophoresis (1%). (b) Second PCR product analysis using gel electrophoresis (1%). VHH fragment with 400-500 bp size is marked

Table 1. Titration results and enrichment of the CD19-specific phages follow biopanning of the nanobody gene library on purified antigen (antigen panning)

Selection round	Input	Out put	Ratio Out /In put	Enrichment ratio
First	1.7 × 10 12	1.2 ×10 7	7×10 -6	1
Second	1.4 × 10 12	1.6 ×10 7	1.1 ×10 -5	1.5
Third	1.9 × 10 12	7.4 ×10 7	3.8 ×10 -5	5.4
Forth	2.3 × 10 12	1.8 ×10 8	7.8 ×10 -5	11
Fifth	2.7 × 10 12	3.9 ×10 8	1.4×10-4	20

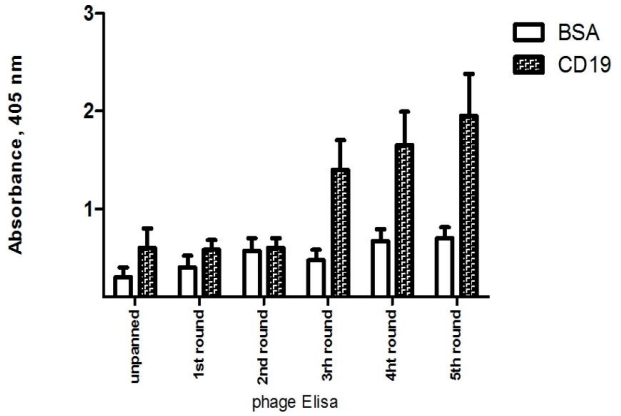

Figure 2. Phage ELISA: Results of anti-CD19 virions after biopanning of the nanobody gene library phages through five panning rounds (fourth and fifth rounds), that yielded the highest signals in ELISA (Kruskal–Wallis one-way analysis of variance, P=0.003) and were used for isolation of anti-CD19 nanobodies. The assay was performed in triplicate and the results are the average of three optical densities (at 450 nm) for each cell line±SD

of the specific binding of each output pooled phage with an anti-M13 antibody further verified the success of the selection process (Figure 2). The yield of the third, fourth, and fifth biopanning rounds was monitored by ELISA for exclusive CD19-specific binders.

Of the total 800 randomly selected colonies, 12 clones showed high-binding ability to the CD19 antigen with very low affinity against BSA. Sequence analysis of positive clones disclosed that 12 unique sequences were verified. Of these 12 clones, 2 clones (i.e., SRB37 and SRB85) showing the highest signal in ELISA were subjected to subsequent analysis (Figure 3 a,b). The amino acid sequences of the two selected clones are confirmed in Table 2 and the algorithms showed a high similarity between human antibodies and SRB-85 and SRB-37 (Max sequence difference was 0.45) (Figure 3 c, d).

Production of soluble nanobodies

Generation of soluble Nbs was carried out after transformation of selected phagemids into *E. coli* TAP10f cells. The expressed proteins were extracted from IPTG-induced cultures of TAP10f by cell sonication and purified by chromatography. In order to support the suitable expression of Nb proteins and to characterize their molecular weight, equal amounts of each Nb samples were resolved by SDS-PAGE under reducing conditions, and then detected via western blotting. Both Nbs were monomeric with the molecular weight of around 14–16 kDa. The expression yield of Nbs varied from 1 to 5 mg/l of culture. But after extraction, Nb was in dimer form. To prevent dimerization, a standard amount of 2-ME was used (Figure 4). The soluble Nbs were analyzed by ELISA for their binding capacity to the CD19 antigen. Both selected Nbs were proven to be specific toward the target protein (CD19) (Figure 4a,b)

Specificity

In an attempt to confirm the specificity of the nominated Nbs, ELISA assay was conducted with serial dilutions of anti-CD19 Nbs. All individual Nbs and mixture of Nbs were highly specific for the CD19 antigen, while the control Nb had no sign of binding to the target (Figure 5a,b,c,d). However, when single

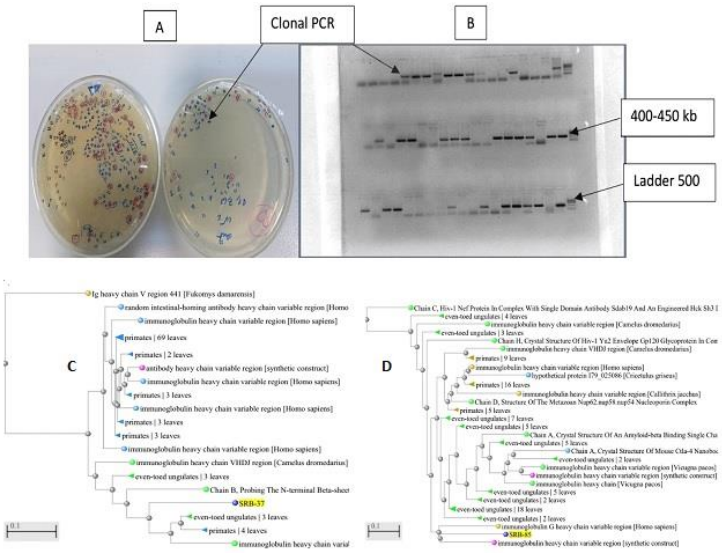

Figure 3. Selection of CD19-specific phage nanobodies (A) clonal selection on the plate (B) clonal PCR and ELISA (C and D), Blast tree SRB-37 and Blast tree SRB85, Neighbor-joining phylogenetic tree of the dromedary germline VH and VHH segments. Database sequences that differed by >7.5% in sequence relative to the mined germline sequences from the RM genome were considered to represent distinct genes. The neighbor joining method is a method for re-constructing phylogenetic trees, and computing the lengths of the branches of this tree. In each stage, the two nearest nodes of the tree (the term "nearest nodes" will be defined in the following paragraphs) are chosen and defined as neighbors in our tree). For purposes of this sequence tree presentation, an implicit alignment between the database sequences is constructed based upon the alignment of those (database) sequences to the query

Table 2. Sequence alignment of the selected anti-CD19 nanobodies with FR1-4 and CDR1-3 the framework regions (FRs) and complementarity determining regions (CDRs) are indicated

Clone	FR1	CDR1	CDR2	FR2
SRB-85	EVQLLESGGGLVQPGGSLRSCEAS	GFN----AMT	SIDS-----WTDAVKG	WVRQPPGKGLEWVS
SRB-37	EVQLQESGGGLVQPGGSLRLSCAAS	GF-----IYMV	GIKTERDG------VKG	WVRQAPGKGLEWLS
Clone	FR3	CDR3	FR4	
SRB-85	RFAISQDNAKNTVYLQMNSLKPEDTAMYYC	AL-----SKCYT---RVYDY	WGQGTQVTVSSG	
SRB-37	RFTIPRDNAKNTLYLQMNNLKSEDTALYYC	ATE---E--ND	WGQGTQVTVSSG	

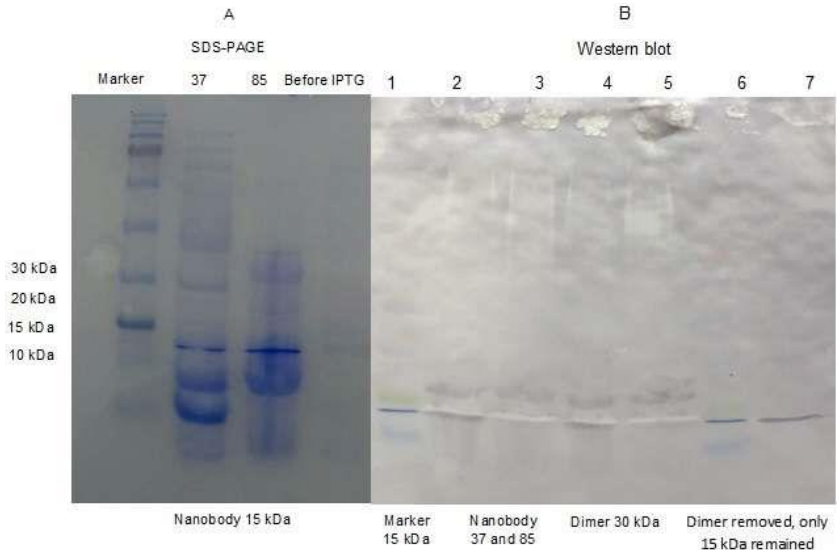

Figure 4. SDS-PAGE and Western blotting analysis; (a) SDS-PAGE gel stained with Coomassie blue; lane marker: MW marker; lane 37 (clone 37) and 85 (clone 38): cell lysate containing expressed VHH following induction with 0.5 mM isopropyl-b-D-thiogalactopyranoside (IPTG); lane before IPTG: bacterial host before induction. (b) lane 1: MW marker; lane 2 and 3: VHH clones 37 and 85 expressed following induction with 0.5 mM IPTG, representing the specific reaction of the horseradish peroxidase (HRP)-conjugated anti-His Tag antibody with nanobodies, which both formed dimer (30kDa) in lanes 2, 3, 4, and 5; lane 6: marker; lane 7: VHH dimer was removed and monomer 15 kDa VHH was purified (4CN Staining)

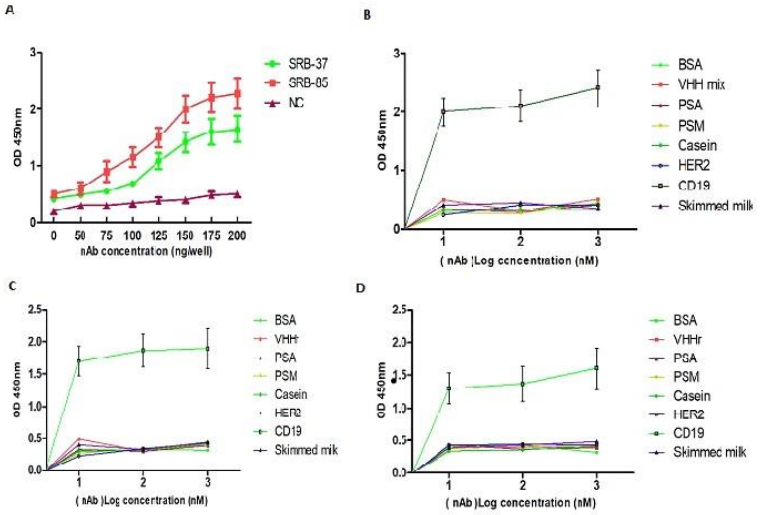

Figure 5. Binding specificity of the anti-CD19 nanobodies. (a) Two selected nanobodies specifically recognized the target antigen and the control nanobody that showed no specificity for CD19 and did not bind to the target antigen. (b) Specific binding of the mixed nanobody (SRB-37 and 85),(C) SRB-37 and (D) SRB-85 to CD19 and other antigens: bovine serum albumin (BSA), VHHr, PSA, porcine submaxillary mucin (PSM), casein, HER2, CD19 and skimmed milk is shown as control factor to confirm that the selected nanobodies were highly specific for the CD19 antigen. Each point is reprehensive of the average of three repetitions±SD

Nbs were incubated with the CD19 antigen, no cross-reactivity was detected with other proteins.

Sensitivity

The binding sensitivity of anti-CD19 Nbs was examined by ELISA (Figure 6). Both selected Nbs

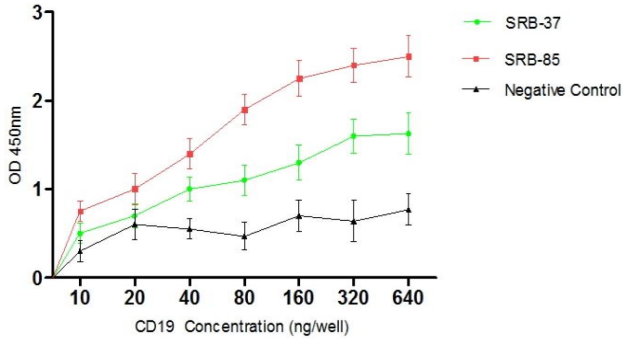

Figure 6. Binding sensitivity of selected nanobodies; The CD19 antigen was coated at different concentrations (0, 10.20, 40, 80, 160, 320, and 640 ng/well); subsequently, SRB-37 and SRB-38 nanobodies (2 µg/ml) and negative control nanobody were added and their binding to CD19 was detected by horseradish peroxidase (HRP)-labeled anti-HA antibody. Each point represents the average of three repetitions±SD

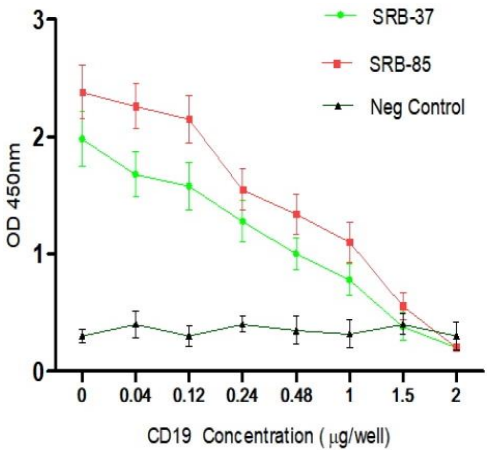

Figure 7. Competitive ELISA: The experiments to determine ability of soluble CD19 antigen to inhibit binding of selected anti-CD19 nanobodies (SRB-37 and SRB-85) and negative control to the coated antigen. Data represents the mean of three repetitions±SD

could quickly bind to the coated CD19 antigen at a concentration of 10 ng/well.

Competition assay

Incubation of the Nb solutions with gradually increasing amounts of the soluble CD19 antigen resulted in blockage of the binding to CD19-coated wells (Figure 7). As depicted in figure 7, the binding blockage pattern of different Nbs differs between the two clones.

Affinity

The binding affinity of the isolated Nbs was specified by enzyme immunoassay, which demonstrated the analysis constants of Nb binders for CD19, arrayed from 15 to 33 nM (Table 3).

Cell ELISA

The Namalwa cell line that expresses the CD19 protein was used to test the immunoreactivity of the selected Nbs against the native form of the antigen. A considerable OD discrepancy between the soluble Nbs and the negative control was indicative of the fact that these Nbs could find the native conformation of CD19 on the surface of the Namalwa cells (Figure 8). Furthermore, combined Nbs in a mixture proved to be more effective than the single Nbs in terms of detecting CD19 on the surface of the B- cells. However, no immunoreactivity was detected against the K562 cell line (CD19 negative cells).

Flow cytometry studies

Raji, Ramos, Namalwa and Daudi cell lines expressing the CD19 protein were utilized for flow cytometry assay to prove binding of the selected Nbs to this antigen. A considerable rightward shifts in the fluorescence peak of the Raji, Ramos, Namalwa, Daudi and the negative control K562 cell lines was observed (Figure 9). When combined SRB-37 and SRB-38 in a mixture were tested, the cocktail could effectively detect CD19 on the surface of the B-cells. However, no immunoreactivity was observed in the K562 cell line (CD19 negative cells). Anti-C19-PE antibody (Becton, Dickinson and Company USA) verified that all tested cell lines with the exception of K562, as control negative, represent over 90 percent expression of the CD19 receptor on their surface.

Table 3. Affinity of anti-CD19 nanobodies

kDa (nM)	CD19 Nanobody
33	SRB-37
15	SRB-85

Discussion

Production of mAb is one of the most advanced technologies in the pharmaceutical industry (35). Monoclonal antibodies are now extensively used to treat various diseases such as immunological disorder and cancer (35). Antibody fragments are now at the focus of most researches since these small molecules have many advantages, and can be used for therapeutic purpose (36). In this study, we employed phage display technology to obtain anti-CD19 specific Nbs from a large one-humped camel derived immune Nb library (37). Thus far, various reports have focused on selection of recombinant antibody fragments specific for CD19 antigen. A brief overview of anti-CD19 mAb can be found on the list such as Blinatumomab, Coltuximabravtansine, MOR208 and MEDI-551 (7). All of these antibodies are at different stages of the clinical trial or in the market, but most of

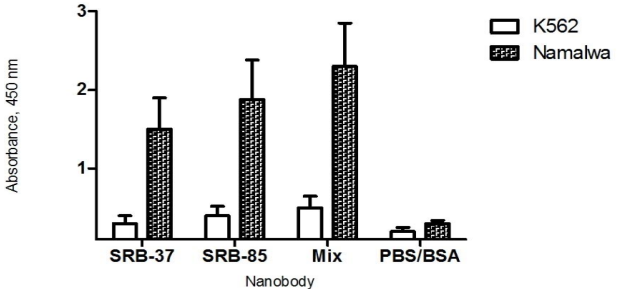

Figure 8. Immunoreactivity of nominated nanobodies toward Namalwa- expressing CD19 cells. The mixture of the two selected nanobodies showed a high signal (Kruskal–Wallis one-way analysis of variance, *P*=0.003). The graph represents a summary of the results of three independent assays

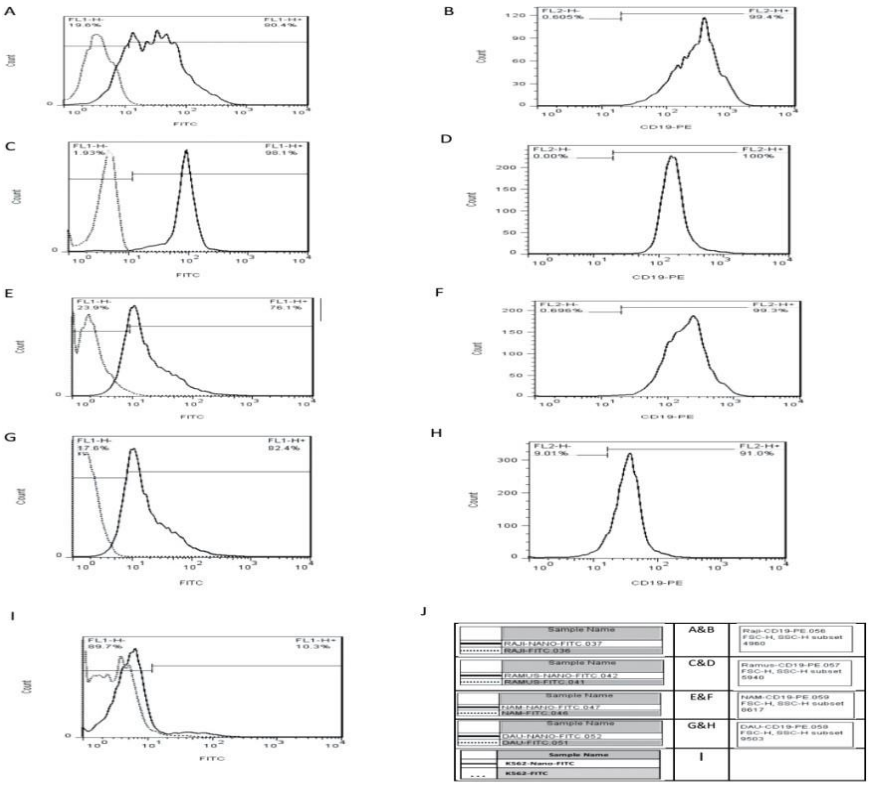

Figure 9. Anti CD19 nanobody specifically binds to antigen-positive cells; (A) Raji cell line with nanobody (SRB-37,85) plus anti-His-FITC (B) Raji anti CD19-PE positive control, (C) Ramos cell line with nanobody (SRB-37,85) plus anti-His-FITC (D) Ramos anti-CD19-PE positive control (E) Namalwa cell line with nanobody (SRB-37,85) plus anti-His-FITC (F) Namalwa anti-CD19-PE positive control (G) Daudi cell line with nanobody (SRB-37,85) plus anti-His -FITC (H) Daudi anti-CD19-PE positive control (I) K562 cell line with nanobody (SRB-37,85) plus anti-His-FITC (J) guide figure line

them have some limiting features such as big size, HAMA generation, and unstable protein structure, which are destroyed following pH and temperature changes. As far as we know, this is the first study, describing anti-CD19 Nbs (VHHs). Since the discovery of camelid heavy-chain antibodies about 20 to 25 years ago, their single-domain antigen-binding fragments also called VHHs or Nbs, have received a progressively increasing interest (12). Having many beneficial properties, Nbs as stable and firm recombinant entities are highly valued proteins for multiple applications, including fundamental research, diagnosis, and therapeutic purposes (38). Due to the distinct Nb-based applications, they are currently undergoing extensive research and development in many applied as therapeutics against extracellular receptors as target(EGFR, HER2, c-MET, VEGFR, DR5, and CXCR4/7), ligands as target (HGF, VEGF, uPA, and CXCL11/12), drug delivery moieties as targets (VEGFR2, EGFR, c-MET, HER2, and MUC1), a particles to deliver (liposomes, micelles, NANAPs, polymersomes, polyplexes, and intrabodies), diagnostic tools such as extracellular receptors **(**AFP, CAIX, PMSA, TAG-72, and HER2) and imaging targets such as PMSA, MMR, HER2, HGF, VCAM1, CAIX, and EGFR (39, 40). Phage-display antibody technology has become increasingly popular for manufacturing binding sites and application in all fields of medical and industrial researches (37). The VHH selected from immunized camels or llamas has possessed some advantages in comparison with the Fab and scFv. VHH technology directly excludes a number of non-specific clones and it is a straightforward method for achieving the target clones (41). As a result of the precise application of camel immunization by B-cells, we could create a very rich library, which is very useful to search for B-cell surface receptors, especially CD19, CD20 and CD21 for targeting B-cell malignancy (such as non-Hodgkin lymphoma), as well as for B-cell autoimmunity (such as systemic lupus erythematosus) (42).

B-cell depletion therapy, administrating mAbs alone or in combination with chemotherapeutic drugs and radiotherapy has exceedingly developed to treat various hematological malignancies and to prolong overall patient survival (43). A promising antibody among the many well-responded mAbs is anti-CD20 (RTX) (42). Anti-CD20 mAbs, particularly RTX have been identified as being deficient due to inducing resistance in patients; therefore, a need for alternative strategies is felt (6). Anti- CD19, another B cell-specific cell surface antigen, can be utilized as a potential complementary to anti-B cell mAbs. CD19 is a B- cell surface receptor whose vast expression, from pre-B cell to early plasma cell, makes it a significant feature for immunotherapy and targeted drug delivery in B-cell malignancies (44). Internalization of this receptor is also favorable for targeted drug delivery. In the present study, we demonstrated that anti-CD19 Nb can effectively target malignant cell lines *in vitro*, which resulted in the introduction of two novel anti-CD19 Nbs, with a small size and high efficacy (45).

A main factor regulating successful tumor targeting by

antibodies is their binding affinity for the target antigen (46), which can determine fundamental properties of mAbs such as cell penetration, localization, specificity, and efficacy (47). In order to achieve high affinity clones, we used very low concentration of the antigen. We managed to isolate a panel of CD19-specific Nbs after the last round of selection, with the affinity of isolated Nbs, estimated at the standard range of 15-35 nM.

Considering the flow cytometry results, the normal expression of CD19 on the B-cell is very different (48).

Our results showed that the cocktail Nb binds to Ramos more than Daudi, Raji and Namalwa cell lines and dose not target the negative control cell line (K562). It should be noted that Ramos cells compared to other cell lines expressed higher levels of CD19 antigen. Target specificity of Nbs without causing any damage to the normal cell is a basic and essential requirement for stringent targeting of the tumors. One of the main achievements of this research was monitoring and repressing a highly specific CD19 receptor by delivering a toxin to tumor B-cells, which will be covered in our future articles.

A major challenge associated with applying murine anti-CD19 and CD20 antibodies is the stimulation of the host immune response such as HAMA generation in a few individuals among the patients (48). Our sequencing results implied high sequence homology (approximately 90%) between the Nb and Homa variable immunoglobulin domains (37). Thus, it may be predicted that potentially low immunogenicity may be induced in human subjects. Another advantage of the Nb that makes it distinguishable from other conventional antibodies is the antigen binding loops (15). The antigen-binding site of Nbs show a much greater structural repertoire that is observed in conventional VH (49). More importantly, the CDR3 regions of Nbs are on average longer than those observed in VH(49, 50). The length of VH amino acids is about 9-12 amino acids, whereas in dromedary derived Nbs, a length of 16-18 amino acids is typically detected. According to our findings, extracted CDR3 region of SRB-37 and SRB-85 Nbs consisted of 9 and 19 amino acids, respectively.

The other advantage of Nbs is their high solubility and stability due to amino acid replacement. Replacing hydrophobic amino acids with their hydrophilic counterparts (V37F or V37Y, G44E, L45R and W47G) within the FR2 region (the residues in this region of the VH are usually connected to the VL domain and are well-conserved through evolution) is a potential solution as demonstrated in our Nbs (Table 2)(49, 50).

Conclusion

This is the first report on the production of nanobody against human CD19. Following *in vivo* analysis, the produced Nbs have the potential to be used as research and diagnostic tools, small molecule drugs and in drug delivery systems against B-cell malignancy and autoimmune disease.

Acknowledgment

The results described in the present paper are part of a PhD thesis supported by Tarbiat Modares University. We would like to thank all staff at the Immunology and Aerobic Bacterial Research and Vaccine Production Department of Razi Institute, Karaj, Iran, Department of Medical Immunology and Department of Medical Biotechnology, School of Medical Sciences, Tarbiat Modares University, for their contribution in conducting this research.

Conflicts of Interest

The authors, hereby, declare that they have no competing interests.

References

1. Zhou L-J, Ord DC, Hughes AL, Tedder TF. Structure and domain organization of the CD19 antigen of human, mouse, and guinea pig B lymphocytes. Conservation of the extensive cytoplasmic domain. J Immunol 1991;147:1424-1432.
2. Park J, editor CD19 CAR therapy for acute lymphoblastic leukemia2015: American Society of Clinical Oncology.
3. Fairfax KA, Tsantikos E, Figgett WA, Vincent FB, Quah PS, LePage M. BAFF-driven autoimmunity requires CD19 expression. J Autoimmun 2015;62:1-10.
4. Benjamini O, Jain P, Trinh L, Qiao W, Strom SS, Lerner S. Second cancers in patients with chronic lymphocytic leukemia who received frontline fludarabine, cyclophosphamide and rituximab therapy: distribution and clinical outcomes. Leuk Lymphoma. 2015;56:1643-1650.
5. Lugtenburg P, Brown PDN, Van der Holt B, D'Amore FA, Koene H, Berenschot H, editors. Randomized phase III study on the effect of early intensification of Rituximab in combination with 2-weekly CHOP chemotherapy flollowed by Rituximab or no maintenance in patients with diffuse large B-cell lymphoma: Results from a HOVON-Nordic Lymphoma Group Study. ASCO Annual Meeting; 2016.
6. Van der Kolk L, Grillo-López A, Baars J, Hack C, Van Oers M. Complement activation plays a key role in the side-effects of rituximab treatment. Br J Haematol 2001;115:807-811.
7. Hansen HJ, Qu Z, Goldenberg DM. Anti-CD19 antibodies. Google Patents; 2017.
8. Velasquez MP, Gottschalk S. Targeting CD19: the good, the bad, and CD81. Blood 2017;129:9-10.
9. Breton CS, Nahimana A, Aubry D, Macoin J, Moretti P, Bertschinger M. A novel anti-CD19 monoclonal antibody (GBR 401) with high killing activity against B cell malignancies. J HEMATOL ONCOL 2014;7:33.
10. Garfall AL, Maus MV, Hwang W-T, Lacey SF, Mahnke YD, Melenhorst JJ. Chimeric antigen receptor T cells against CD19 for multiple myeloma. N Engl J Med. 2015;373(11):1040-7.
11. Katz B-Z, Herishanu Y. Therapeutic targeting of CD19 in hematological malignancies: past, present, future and beyond. Leuk Lymphoma 2014;55:999-1006.
12. De Meyer T, Muyldermans S, Depicker A. Nanobody-based products as research and diagnostic tools. Trends Biotechnol. 2014;32:263-270.
13. Honda T, Akahori Y, Kurosawa Y. Methods of constructing camel antibody libraries. Google Patents; 2008.
14. Harmsen M, De Haard H. Properties, production, and applications of camelid single-domain antibody fragments. Appl Microbiol Biotechnol. 2007;77:13-22.
15. Könning D, Zielonka S, Grzeschik J, Empting M, Valldorf B, Krah S. Camelid and shark single domain antibodies: structural features and therapeutic potential. Curr Opin Struct Biol. 2017;45:10-6.
16. Wang Y, Fan Z, Shao L, Kong X, Hou X, Tian D. Nanobody-derived nanobiotechnology tool kits for diverse biomedical and biotechnology applications. Int J Nanomedicine. 2016;11:3287.
17. van Lith SA, Roodink I, Verhoeff JJ, Mäkinen PI, Lappalainen JP, Ylä-Herttuala S. In vivo phage display screening for tumor

vascular targets in glioblastoma identifies a llama nanobody against dynactin-1-p150 Glued. Oncotarget. 2016;7:71594-71607.
18. Veugelen S, Dewilde M, De Strooper B, Chávez-Gutiérrez L. Chapter Three-Screening and Characterization Strategies for Nanobodies Targeting Membrane Proteins. Methods Enzymol 2017;584:59-97.
19. Sharifzadeh Z, Rahbarizadeh F, Shokrgozar MA, Ahmadvand D, Mahboudi F, Jamnani FR. Development of oligoclonal nanobodies for targeting the tumor-associated glycoprotein 72 antigen. Mol Biotechnol 2013;54:590-601.
20. Ahmadvand D, Rasaee MJ, Rahbarizadeh F, Kontermann RE, Sheikholislami F. Cell selection and characterization of a novel human endothelial cell specific nanobody. Mol Immunol 2009;46:1814-1823.
21. Rahbarizadeh F, Rasaee MJ, Forouzandeh M, Allameh A-A. Over expression of anti-MUC1 single-domain antibody fragments in the yeast Pichia pastoris. Mol Immunol. 2006;43:426-435.
22. Hoogenboom HR, Lutgerink JT, Pelsers MM, Rousch MJ, Coote J, van Neer N Selection-dominant and nonaccessible epitopes on cell-surface receptors revealed by cell-panning with a large phage antibody library. Eur J Biochem. 1999;260:774-784.
23. Jamnani FR, Rahbarizadeh F, Shokrgozar MA, Ahmadvand D, Mahboudi F, Sharifzadeh Z. Targeting high affinity and epitope-distinct oligoclonal nanobodies to HER2 over-expressing tumor cells. Exp Cell Res. 2012;318(10):1112-24.
24. Desper R, Gascuel O. Theoretical foundation of the balanced minimum evolution method of phylogenetic inference and its relationship to weighted least-squares tree fitting. Mol Biol Evol. 2004;21:587-598.
25. Gazarian T, Selisko B, Hérion P, Gazarian K. Isolation and structure–functional characterization of phage display library-derived mimotopes of noxiustoxin, a neurotoxin of the scorpion Centruroides noxius Hoffmann. Mol Immunol. 2000;37:755-766.
26. Kay BK, Winter J, McCafferty J. Phage display of peptides and proteins: a laboratory manual: Academic Press; 1996.
27. Bradford MM. A rapid and sensitive method for the quantitation of microgram quantities of protein utilizing the principle of protein-dye binding. Anal Biochem 1976;72:248-254.
28. Dumoulin M, Conrath K, Van Meirhaeghe A, Meersman F, Heremans K, Frenken LG. Single-domain antibody fragments with high conformational stability. Protein Sci 2002;11:500-515.
29. Laemmli UK. Cleavage of structural proteins during the assembly of the head of bacteriophage T4. nature. 1970;227:680-685.
30. Engvall E. Enzyme immunoassay ELISA and EMIT. Methods Enzymol. 1980;70:419-439.
31. Rameh LE, Arvidsson A-k, Carraway KL, Couvillon AD, Rathbun G, Crompton A. A comparative analysis of the phosphoinositide binding specificity of pleckstrin homology domains. J Biol Chem. 1997;272:22059-22066.
32. Ghassabeh GH, Saerens D, Muyldermans S. Isolation of antigen-specific nanobodies. Antibody engineering 2010:251-266.
33. Beatty JD, Beatty BG, Vlahos WG. Measurement of monoclonal antibody affinity by non-competitive enzyme immunoassay. J Immunol Methods 1987;100:173-179.
34. Loken MR, Shah VO, Dattilio KL, Civin CI. Flowcytometric analysis of human bone marrow. II. Normal B lymphocyte development. Blood. 1987;70:1316-1324.
35. Nelson AL, Dhimolea E, Reichert JM. Development trends for human monoclonal antibody therapeutics. Nat Rev Drug Discov. 2010;9:767-774.
36. Morrow KJ, Liu C. Biosimilars of Monoclonal Antibodies: A Practical Guide to Manufacturing, Preclinical and Clinical Development: John Wiley & Sons; 2016.
37. Clackson T, Hoogenboom HR. Making antibody fragments using phage display libraries. Nature 1991;352:624.
38. Muyldermans S, Baral T, Retamozzo VC, De Baetselier P, De Genst E, Kinne J. Camelid immunoglobulins and nanobody technology. Vet Immunol Immunopathol 2009;128:178-183.
39. Van Audenhove I, Gettemans J. Nanobodies as versatile tools to understand, diagnose, visualize and treat cancer. EBioMedicine 2016;8:40-48.
40. Farajpour Z, Rahbarizadeh F, Kazemi B, Ahmadvand D. A nanobody directed to a functional epitope on VEGF, as a novel strategy for cancer treatment. Biochem Biophys Res Commun 2014;446(1):132-136.
41. Drive R, entitled DDEIaptsaora, B-Lymphocyte DoSCNVfCI-toH, disclose. TmhnbpainucfpeWhncoit, Co-author:, *et al*. Evaluation of a nanobody phage display library constructed from a Brucella-immunised camel. Vet Immunol Immunopathol. 2011;142:49-56.
42. Czuczman M, Grillo-Lopez A, White C, Saleh M, Gordon L, LoBuglio A. Treatment of patients with low-grade B-cell lymphoma with the combination of chimeric anti-CD20 monoclonal antibody and CHOP chemotherapy. J Clin Oncol 1999;17:268-276.
43. Reff ME, Carner K, Chambers K, Chinn P, Leonard J, Raab R. Depletion of B cells in vivo by a chimeric mouse human monoclonal antibody to CD20. Blood. 1994;83:435-445.
44. Schwemmlein M, Stieglmaier J, Kellner C, Peipp M, Saul D, Oduncu F, et al. A CD19-specific single-chain immunotoxin mediates potent apoptosis of B-lineage leukemic cells. Leukemia. 2007;21:1405-1412.
45. Hammer O, editor CD19 as an attractive target for antibody-based therapy. MAbs; 2012: Taylor & Francis.
46. Holliger P, Hudson PJ. Engineered antibody fragments and the rise of single domains. Nat Biotechnol 2005;23:1126-1136.
47. Adams GP, Schier R, McCall AM, Simmons HH, Horak EM, Alpaugh RK. High affinity restricts the localization and tumor penetration of single-chain fv antibody molecules. Cancer Res 2001;61:4750-4755.
48. Henderson A, Ripley S, Heller M, Kieff E. Chromosome site for Epstein-Barr virus DNA in a Burkitt tumor cell line and in lymphocytes growth-transformed in vitro. Proc Natl Acad Sci. 1983;80:1987-1991.
49. Desmyterl A, Transuei TR, Ghahroudil MA, Thil M-HD, Poortmans F, Hamersz R. Crystal structure of a camel single—domain VH antibody fragment in complex. Nat Struct Biol 1996;3:803-811.
50. Vu KB, Ghahroudi MA, Wyns L, Muyldermans S. Comparison of llama VH sequences from conventional and heavy chain antibodies. Mol Immunol 1997;34:1121-1131.